JMEPEG (2007) 16:185–191
DOI: 10.1007/s11665-007-9030-6

1059-9495/$19.00

Superplastic Behavior of Copper-Modified 5083 Aluminum Alloy

Ravi Verma and Sooho Kim

(Submitted April 20, 2006; in revised form October 22, 2006)

An AA5083 aluminum alloy was modified with two different levels of Cu additions, cast by direct-chill method, and thermo-mechanically processed to sheet gauge. Copper additions reduced sheet grain size, decreased tensile flow stress and significantly increased tensile elongation under most elevated temperature test conditions. The high-Cu (0.8 wt.%) alloy had the finest grain size 5.3 μm, a peak strain-rate sensitivity of 0.6 at a strain-rate of 1×10^{-2} s^{-1}, and tensile elongation values between 259 and 584% over the temperature range, 400-525 °C, and the strain rate range, 5×10^{-4} to 1×10^{-2} s^{-1}, investigated. In biaxial pan forming tests, only the Cu-containing alloys successfully formed pans at the higher strain rate 10^{-2} s^{-1}. The high-Cu alloy showed the least die-entry thinning. Comparison of ambient temperature mechanical properties in O-temper state showed the high-Cu alloy to have significantly higher yield strength, ultimate strength, and ductility compared to the base 5083 alloy.

Keywords 5083 aluminum, Cu modified, QPF, superplastic forming, superplasticity

1. Introduction

Use of aluminum in automobile body closures and structures is a key enabler to reduce vehicle mass and improve fuel efficiency. Aluminum's limited formability compared to drawing quality steel, however, has hampered its penetration in the body closure and structure applications. Stamping difficulties associated with the poor ductility, result in increased part count and higher assembly costs of aluminum sheet parts.

Superplastic forming (SPF) is often used to form complex aluminum sheet parts in the aerospace industry (Ref 1, 2). In recent years, SPF has also been used to form automotive aluminum panels for low volume, niche applications (Ref 3-6). Transition of this technology to high volume applications, such as in the mainstream automotive industry, requires a shift from the aerospace paradigm of low initial investment and high piece cost to one of high initial investment and low piece cost. Volume production requires forming at much faster rates and lower temperatures than typically used in SPF. General Motor's quick plastic forming (QPF) technology (Ref 7, 8), unveiled in 2004 (Ref 9), answers this need by optimizing and reengineering all aspects of SPF technology for high volume production. This included development of a low-cost AA5083 aluminum sheet optimized for QPF forming conditions (Ref 10, 11). Such a low-cost sheet is currently being used to produce the Chevrolet Malibu Maxx liftgate and the Cadillac STS decklid.

This article was presented at the AeroMat Conference, International Symposium on Superplasticity and Superplastic Forming (SPF) held in Seattle, WA, June 6-9, 2005.

Ravi Verma, and **Sooho Kim,** General Motors R & D Center, 30500 Mound Road, Warren, MI. Contact e-mail: ravi.verma@gm.com.

Superplastic characteristics of AA5083 have been investigated extensively, and high tensile elongations have been reported for the SPF-grade 5083 alloy at 500-525 °C and strain rates of 1-2 $\times10^{-4}$/s (Ref 12-15). These forming strain rates are much too slow, and further improvements are needed to increase part production rate and make the technology more cost effective. In recent years, particular interest has been focused on alloy chemistry modifications to improve superplastic formability of aluminum sheet (Ref 16-18). Minor additions of Cu, Mn, Cr and Zr to base 5083 aluminum have been shown to improve these properties (Ref 13, 17, 18). The objective of the current study was to investigate and understand the effect of Cu additions on both elevated temperature formability and ambient temperature mechanical properties of AA5083 alloy.

2. Experimental

2.1 Materials

Chemical compositions of the alloys used in this study are given in Table 1. The base alloy is an AA5083 with 0.2% Zr added for potential effect on grain boundary pinning during SPF (Ref 18). The low-Cu and the high-Cu alloys are the Cu-modified versions of the Base alloy, containing 0.40% and 0.78% Cu, respectively. The concentrations of impurity elements, Fe and Si, were significantly below those in a typical commercial 5083 aluminum alloy.

The alloys were cast by the direct-chill (DC) process and rolled to sheet gauge at Kaiser Center for Technology, Pleasanton, CA. Cast ingots, 76 mm thick, were first scalped to a thickness of about 64 mm to remove surface oxides and contaminants. The scalped ingots were homogenized at 510 °C for 10 h, hot-rolled at 510-400 °C (start and end temperatures) to a thickness of 25 mm, then annealed at 540 °C for 24 h, and further hot-rolled at 510-400 °C to a thickness of 10 mm. This was followed by cold rolling 80% to a final sheet thickness of 2 mm.

2.2 Metallographic Preparation

Sheet samples were annealed at 500 °C for 15 min to develop a recrystallized microstructure similar to that which develops at the SPF temperature, prior to the start of forming. The samples were aged at 150 °C for 24 h, and then mounted, polished, and etched by immersing in 10% phosphoric acid at 50 °C for 3-5 min. Grain size was measured by taking the geometric mean of average linear intercepts measured along the rolling (L) and the short-transverse (ST) directions.

2.3 Room Temperature Mechanical Testing

Tensile specimens per ASTM Standard E8 specifications were machined from the base and the high-Cu alloys in the pre- and post-form conditions with the tensile axis parallel to the sheet rolling direction. The specimens had an overall length of 203.2 mm, with a gage section 50.8 mm in length and 12.7 mm in width. Prior to testing, the pre-form specimens were annealed at 500 °C for 15 min to obtain the fully annealed condition similar to one prevailing just prior to superplastic forming at elevated temperature. Ambient temperature tensile tests were performed in an Instron machine equipped with a strain gage.

2.4 High Temperature Tensile Testing

Tensile specimens with a gage section 25 mm in length and 6.35 mm in width were machined from the sheet alloys with the tensile axis parallel to the sheet rolling direction. Tensile tests were performed in an Instron machine equipped with an air-circulating furnace. Samples were heated to the test temperature in about 15 min. Tests were performed at temperatures from 400 to 525 °C, and initial strain-rates from 5×10^{-4} to 1×10^{-2} s^{-1}. Three tests were conducted at each condition. The reported elongation values are an average of the three identical tests. Incremental step-strain-rate tests were conducted at 450, 475, and 500 °C, covering strain-rates from 5×10^{-5} to 1×10^{-2} s^{-1}, to compute materials strain-rate sensitivity of flow stress.

Table 1 Chemical compositions (wt. %) of 5083 aluminum alloys used in the study

Alloy ID	Mg	Mn	Cr	Cu	Zr	Fe	Si
Base	4.72	0.77	0.18	**0.00**	0.21	0.09	0.04
Low-Cu	4.76	0.77	0.18	**0.40**	0.19	0.07	0.04
High-Cu	4.74	0.72	0.18	**0.78**	0.19	0.07	0.04

2.5 Biaxial Forming

Biaxial formability of the sheet alloys was tested by gas-pressure blow forming a rectangular pan, 50 mm wide × 150 mm long × 50 mm deep. A pressure-time cycle, computed based on a plane-strain forming model was used to form the pans (Ref 19, 20).

3. Results and Discussion

3.1 Microstructure

Figure 1 shows microstructures of the sheet alloys in the recrystallized (fully annealed) state. All three alloys exhibit highly refined grain structure with an average grain size between 5.3 and 6.0 μm. Generally the Cu-containing alloys show a more equiaxed grain structure than the base alloy. The high-Cu alloy has the finest grain size (5.3 μm), suggesting potentially high superplastic formability.

3.2 Elevated Temperature Tensile Behavior

Effects of alloy chemistry, test temperature, and strain-rate on tensile elongation of AA5083 alloy are shown in Fig. 2. Both Cu-containing alloys show significantly higher tensile elongations than the base alloy, under all test conditions investigated. The high-Cu alloy shows higher elongation than the low-Cu alloy in seven out of nine test conditions investigated. At 475 °C, the high-Cu alloy exhibits the highest elongations of all alloys with consistently high elongation values (430-474%) over the strain-rates investigated. The increase in elongation due to 0.8% Cu addition is highest at strain rate 1×10^{-3} s^{-1}; the exact increase depending upon the test temperature. For example, at 475 °C the elongation increases from 240% in the case of the base alloy, and to 450% in case of the high-Cu alloy. At the highest strain-rate 1×10^{-2} s^{-1}, the elongations of the two Cu containing alloys are very comparable at 500 °C and 525 °C.

The effects of Cu on the flow stress (0.2% offset) and the peak stress of AA5083 alloy, at a strain rate of 3×10^{-3} s^{-1}, are shown in Fig. 3. Both decrease with increasing test temperature, and increasing Cu content. The lowest strength values were observed for the high-Cu alloy. The drop in strength is the highest going from 0.4% to 0.8% Cu at 475 °C.

3.3 SPF Characterization of High-Cu Alloy

Since the high-Cu alloy exhibited the highest tensile elongation, the alloy's deformation behavior was further investigated, over wide temperature and strain-rate ranges.

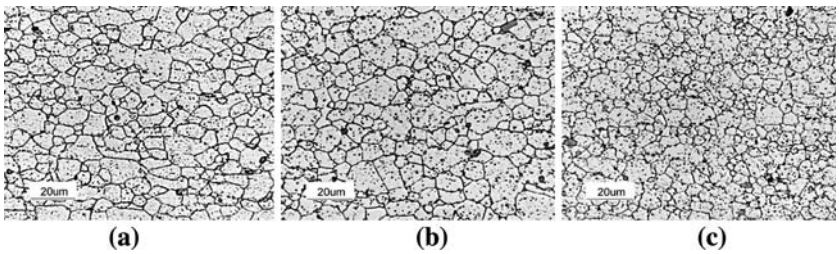

Fig. 1 Optical micrographs of recrystallized sheet alloys, (a) base 5083, (b) base + 0.4%Cu, and (c) base + 0.78%Cu

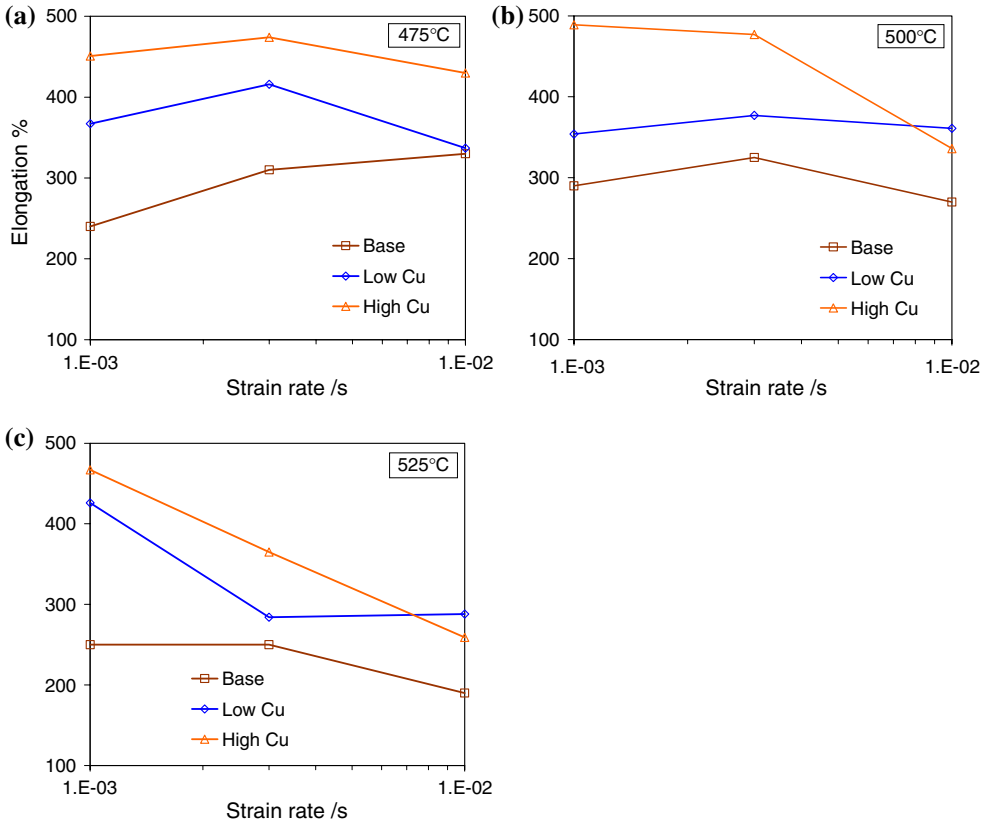

Fig. 2 Effect of strain-rate on tensile elongation of alloys at (a) 475 °C, (b) 500 °C, and (c) 525 °C

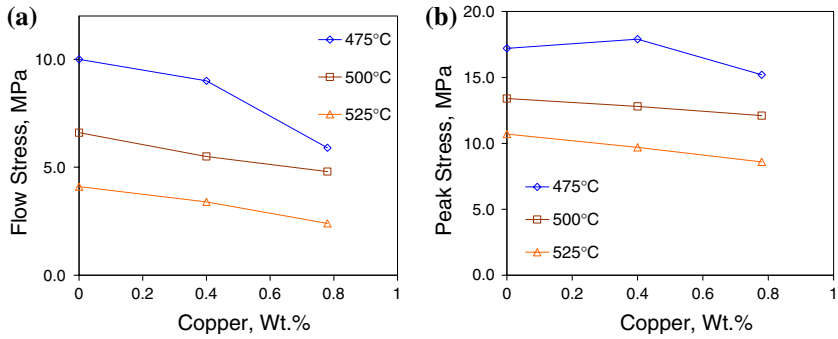

Fig. 3 Effect of Cu addition on flow stress (a) and peak stress (b) of AA 5083 alloy tested at 3×10^{-3} s^{-1} initial strain rate

The tensile elongation results are plotted as a function of strain rate in Fig. 4a, and as a function of temperature in Fig. 4b. In general, elongation decreases with increasing strain rate at all temperatures, but more slowly in the mid temperature range (425-475 °C).

The elongation peaks in the neighborhood of 450-475 °C (Fig. 4b) for all strain rates. The highest elongation of 584% occurs at 450 °C and 1×10^{-3} s^{-1}. This is an unusually low temperature for high ductility in superplastic AA 5083. The deformation at 450 °C and 1×10^{-3} s^{-1}, as seen in Fig. 5, is superplastic in nature with the specimen tested showing very uniform deformation through the entire gage section. It appears that Cu addition may have a role in lowering the optimum superplastic temperature of the high-Cu alloy. The alloy shows a wide forming window with elongation equal to or more than about 400% at all strain rates, including the highest 10^{-2} s^{-1}, in the temperature range 425-475 °C. Elongation values over the GM specification of 325% (Ref 21) occur in 27 out of 29 temperature and strain-rate combinations investigated.

Incremental step-strain-rate tests were conducted at 450, 475, and 500 °C, covering strain-rates from 5×10^{-5} to 1×10^{-2} s^{-1}. Figure 6a shows flow stress as a function of strain-rate for different test temperatures. The plots have the typical sigmoidal shape indicative of different creep phenomena operating in different strain-rate regimes. Grain-boundary sliding dominates in the intermediate strain-rate range (slope ≅0.5) (Ref 22, 23). At higher strain-rates, solute-drag-creep increasingly replaces grain-boundary-sliding as the main deformation process, as indicated by the decreasing slope in Fig. 6a (Ref 22, 23). The plot slope represents strain-rate sensitivity

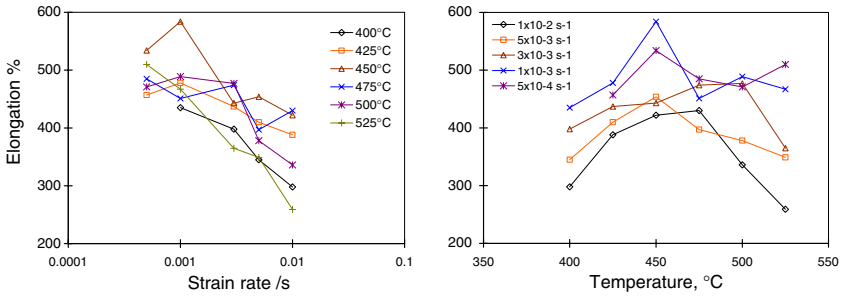

Fig. 4 Tensile elongation of high-Cu alloy, (a) as a function of strain rate at different temperatures, and (b) as a function of temperature at different strain rates

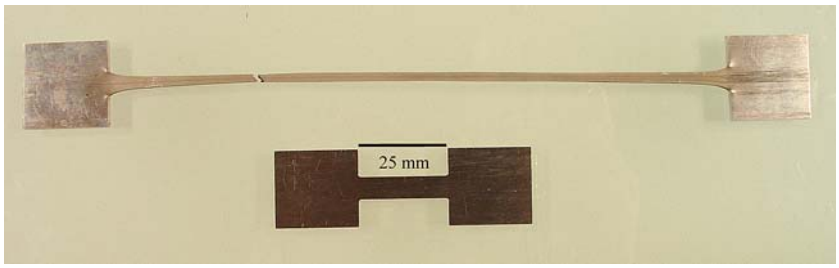

Fig. 5 High-Cu alloy tensile specimen tested to failure at 450 °C and 1×10^{-3} s^{-1}. Also shown is an untested specimen

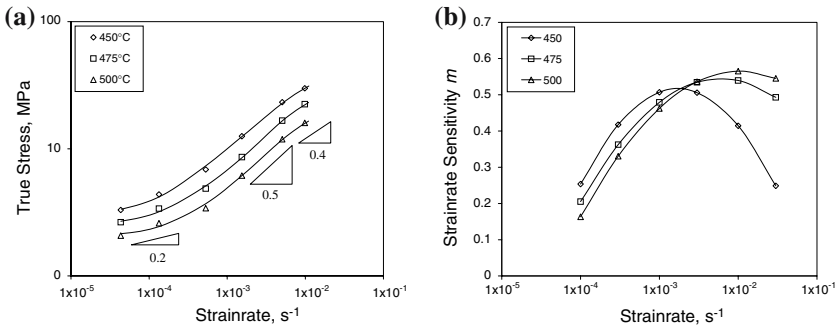

Fig. 6 High-Cu alloy; flow stress (a) and strain-rate sensitivity *m* (b) as a function of strain-rate

index, *m*, of the material, and is plotted as a function of strain-rate in Fig. 6b. The *m* plots have the typical bell shape, with the peak *m* values of over 0.5, indicating high formability at all three temperatures. The peak *m* occurs at increasingly higher strain-rates with increasing test temperature. A temperature increase from 450 to 500 °C increases the "peak" strain rate from 1×10^{-3} to 1×10^{-2} s^{-1}. In contrast, a base 5083 alloy has been shown to display peak *m* at strain-rates between 5×10^{-4} and 1×10^{-3} s^{-1} (Ref 24, 25). These results indicate that the high-Cu alloy can be formed 10× faster than a base 5083 aluminum alloy.

3.4 Cu-Containing Grain-Boundary Phase

Attempts to test the Cu-containing alloys at or above 550 °C resulted in incipient melting. Similar incipient melting in Cu-modified AA5083 alloy has been observed by others (Ref 26). The incipient melting is most likely due to a low-melting intermetallic phase at the alloy grain boundaries. Transmission electron microscopy (TEM) investigation of the alloys (Ref 27) showed intermetallic particles with two distinct morphologies: coarser, rod-like particles, of size in the 0.2-0.4 μm range, and much finer, spherical shaped particles of size in the 30-50 nm range. The rod-like particles, fairly uniformly distributed in the alloy matrix, appeared to be an Al_6Mn-type phase. The fine spherical particles tended to cluster along the grain-boundaries in the form of a network, and had significant amounts of Mg and Cu with rest Al (Al-Mg-Cu). Based on the Cu-Mg binary system (Ref 28), it appears that the Al-Mg-Cu phase in the Cu-containing alloys may be the low-melting intermetallic phase responsible for the incipient melting. Further work is needed to confirm this assertion. Since diffusivity scales with melting temperature, a low-melting phase can enhance diffusivity even at temperatures below the incipient melting temperature. It appears that the low-melting phase at the grain boundaries, through enhancement of grain boundary sliding, is responsible for the lower flow stress and increased elongation in the Cu-containing alloys.

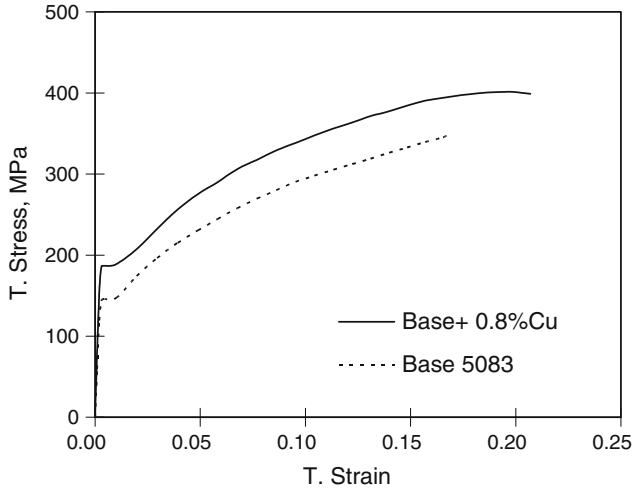

Fig. 7 True stress-true strain plots of alloys in the recrystallized state

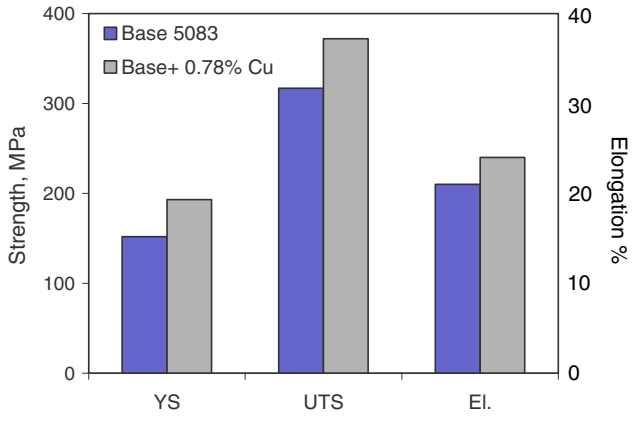

Fig. 8 Mechanical properties of base 5083 and base + 0.78%Cu alloys in the recrystallized state

3.5 Mechanical Properties

Ambient temperature tensile test results of the base and the high-Cu alloys in the fully annealed (pre-form) condition are plotted in Fig. 7 and 8. Both alloys show a high level of strain hardening and little post-uniform elongation in the true stress-strain plots in Fig. 7. The bar chart in Fig. 8 shows significant increase of mechanical properties as a result of the 0.78% Cu addition to base 5083 alloy, with increases of YS from 152 to 193 MPa, UTS from 317 to 372 MPa, and elongation from 18 to 23%. These enhanced mechanical properties are an additional benefit of the Cu-modification of base 5083 alloy, which can have a significant impact on designing lighter aluminum sheet parts with better crash performance.

The sheet materials were also tested in post-SPF condition by taking samples from the bottom of a rectangular pan formed with the two materials, as described in the next section. The pan bottom had a true thickness strain of about −0.35 (thickness reduction 30%) in both cases. The pre- and post-form properties in Table 2 show a slight reduction in the properties after forming, but the benefit of the Cu addition is retained in the post-form material.

Table 2 Mechanical properties of the base and high-Cu alloys in the pre- and post-form conditions

	Pre-form		Post-form	
Property	**Base**	**High-Cu**	**Base**	**High-Cu**
YS, MPa	152	193	138	186
UTS, MPa	317	372	296	345
Elong., %	21	24	18	21

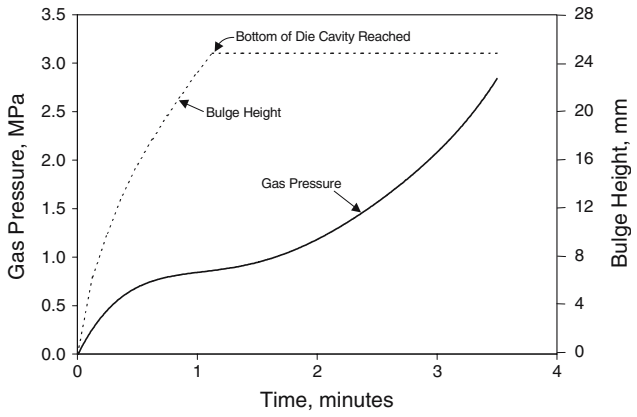

Fig. 9 Gas pressure cycle used to form pan at 500 °C and 5×10^{-3} s^{-1}. Also shown is increase of bulge height with time

3.6 Biaxial Formability

A long rectangular pan tool was used to assess formability of the alloys. The large length-to-width ratio of the pan presents a situation where sheet stretching occurs essentially along the pan width. A long rectangular pan tool was used to assess formability of the alloys. The large length-to-width ratio of the pan presents a situation where sheet stretching occurs essentially along the pan width. This geometry permits a simple plane-strain state to be assumed for modeling sheet formability (Ref 19). The gas pressure/time cycle is computed based on the alloy's stress-strain relationship for the strain-rate of interest, and on the instantaneous thickness and radius of curvature of the sheet in the free forming region. Figure 9 shows a gas pressure-time cycle for forming with the high-Cu alloy at 500 °C and 5×10^{-3} s^{-1}. Also shown in the figure is the bulge height as a function of the forming time. The height stops increasing when the sheet touches the die bottom. This coincides with the point of inflection in the pressure-time plot, after which the pressurization rate continuously increases to maintain the forming strain rate in the increasingly narrower corner regions of the die.

Figure 10 shows a half section of a "fully" formed pan made with the high-Cu alloy. A pan was considered "fully" formed when the bottom pan radius (at mid point on the bottom long edge) was ≤3 mm. Table 3 summarizes forming results in terms of the ability of each alloy to fully form the pan under different forming conditions. The base 5083 alloy was successful in fully forming the pan in two out of four conditions, both associated with the lower strain rate 5×10^{-3} s^{-1}. At the higher strain rate of 1×10^{-2} s^{-1}, the sheet ruptured prematurely at both forming temperatures investigated. With the Cu-containing alloys, it was possible to fully form pans under all

Fig. 10 Pan (half section shown) formed with alloy high-Cu alloy, at 500 °C and 5×10^{-3} s^{-1} strain-rate

Table 3 Pan forming results under different forming conditions

	500 °C		450 °C	
Alloy, strain rate	5×10^{-3} s^{-1}	1×10^{-2} s^{-1}	5×10^{-3} s^{-1}	1×10^{-2} s^{-1}
Base	Complete	*Rupture*	Complete	*Rupture*
Low-Cu	Complete	Complete	Complete	Complete
High-Cu	Complete	Complete	Complete	Complete

Table 4 Formability of alloys at 500 °C

	Alloys		
Formability	**Base**	**Low-Cu**	**High-Cu**
Tensile elongation, % (strain rate: 3×10^{-3} s^{-1})	325	377	425
Normalized sheet thickness at pan entry radius, t_r/t_o (strain rate: 5×10^{-3} s^{-1})	0.28	0.40	0.54

four forming conditions. In fully formed pans made with the three alloys, formability was differentiated in terms of the degree of sheet thinning at the die entry radius, a precursor to sheet rupture. Table 4 compares thinning of the alloy sheets at the die-entry radius with their tensile elongations at 500 °C and 3×10^{-3} s^{-1}. Thinning is expressed in terms of the complimentary term, normalized sheet thickness, t_r/t_o, where t_r is the minimum sheet thickness at the die entry radius and t_o is the initial sheet thickness. The die-entry sheet thinning values track well with alloys' tensile elongation values. The high-Cu alloy, with the highest tensile elongation, shows the least thinning (high thickness ratio), where as the base 5083 alloy, with the lowest tensile elongation, showed the most thinning (low thickness ratio).

4. Conclusions

1. Three alloys, a base AA5083 (base), a 0.4% Cu containing 5083 (low-Cu), and a 0.78% Cu containing 5083 (high-Cu), were investigated.
2. The thermomechanical rolling process used to process cast ingots to sheet gage provided highly refined and equiaxed grain structures with an average grain size of 5-6 μm in all three alloys.
3. The high-Cu alloy showed the highest tensile elongation and lowest flow stress under most temperature and strain rate conditions.
4. Strain-rate sensitivity of the high-Cu alloy peaked at 1×10^{-2} s^{-1} strain-rate, which is an order of magnitude higher than the peak strain-rate in a conventional superplastic-grade 5083 aluminum alloy, suggesting that faster forming with the high-Cu alloy may be possible.
5. At ambient temperature, the high-Cu alloy was significantly stronger and more ductile than the base alloy, which should benefit part design and performance.
6. Only the Cu-containing alloys produced fully formed pans at the higher strain-rate of 1×10^{-2} s^{-1}. The base alloy ruptured prematurely at the higher strain-rate.
7. The high-Cu alloy showed the least thinning (46%, compared to 72% for the base alloy) at the die-entry radius.

Acknowledgments

The authors thank Roy Sexton for help with testing of the alloys, and Dick Hammar and Paul Krajewski for reviewing the manuscript.

References

1. D. Stephen, AGARD Lecture Series No.154, Superplasticity, NATO, 1987, p 1
2. O.D. Sherby and J. Wadsworth, Superplasticity in Aerospace, H.C. Heikkenen and T.R. McNelley Ed., The Metallurgical Society, Warrendale, PA, 1988, p 3
3. A.J. Barnes, 23rd Annual Aluminum Design and Fabrication Seminar, Livonia, MI., 2002
4. A.J. Barnes, *Mat. Sci. Forum*, 1999, **304–306**, p 785
5. Y. Onishi, *Mat. Sci. Forum*, 1999, **304–306**, p 819
6. J.C. Benedyk, *Light Met. Age*, 2002, p 28
7. M.S. Rashid, C. Kim, E.F. Ryntz, F.I. Saunders, R. Verma, and S. Kim, Quick Plastic Forming of Aluminum Alloy Sheet Metal, U.S. Patent 6,253,588, 3 July, 2001
8. J.G. Schroth, "General Motors' Quick Plastic Forming Process," Advances in Superplasticity and Superplastic Forming, E.M. Tallef et al. Ed., TMS, Warrendale, PA, 2004, p 9
9. B. Corbett, "New GM Process Boost to Aluminum," WardsAuto.com, Jan 30 2004
10. R. Verma, unpublished work, 1996
11. R. Verma, "Rolling Process Optimization for Superplastic 5083 Al Sheet," Advances in Superplasticity and Superplastic Forming, E.M. Tallef et al. Ed., TMS, Warrendale, PA, 2004, p 159–170
12. D.J. Lloyd, *Met. Trans.*, 1980, **11A**, p 1287
13. H. Watanabe, K. Ohori, and Y. Takeuchi, *Trans. Iron Steel Inst. Japan*, 1987, **27**, p 730
14. H. Iwasaki, K. Higashi, S. Tanimura, T. Komatubara, and S. Hayami, Superplasticity in Advanced Materials, S. Hori, M. Tokizane, and N. Furushiro Ed., The Japan Society for Research on Superplasticity, 1991, p 447
15. H. Imamura and N. Ridley, Superplasticity in Advanced Materials, S. Hori, M. Tokizane, and N. Furushiro Ed., The Japan Society for Research on Superplasticity, 1991, p 453
16. M.J. Stowell and B.M. Watts, U.S. Patent 4,108,691, 1978
17. H. Iwasaki, Y. Masaki, K. Higashi, S. Tanimura, T. Ito, and S. Hayami, *Journal of JSTP*, 1992, **33**(372), p 87
18. J. S. Vetrano, C.A. Lavender, C.H. Hamilton, M.T. Smith, and S.M. Bruemmer, *Scrip. Metall. Mater.*, 1994, **30**, p 565

19. A.K. Ghosh and C.H. Hamilton, Process Modeling Fundamentals and Applications to Metals, American Society for Metals, 1980, p 303
20. R. Verma, P.A. Friedman, A.K. Ghosh, C. Kim, and S. Kim, "Superplastic Forming Characteristics of Fine-Grained 5083 Aluminum", *J. Mater. Eng. Perform.*, 1995, **4**, p 543
21. R. Verma, "General Motors Alloy Specifications for QPF AA5083 Aluminum Sheet", Unpublished Specifications: QPF AA 5083 H175 DC, October 2000
22. M.-A. Kulas, P.E. Krajewski, T.R. McNelley, and E.M. Taleff, "Deformation and Failure Mechanisms in Commercial AA5083 Materials," Hot Deformation of Aluminum Alloys III, Z. Jin et al. Ed., 2003, p 499
23. E.M. Taleff, P.J. Nevland, and P.E. Krajewski, Tensile Ductility of Several Commercial Aluminum Alloys at Elevated Temperatures, *Metall. Mater. Trans.*, 2001, **32A**, p 1119
24. R. Verma, P.A. Friedman, A.K. Ghosh, S. Kim, and C. Kim, Characterization of Superplastic Deformation Behavior of a Fine Grain 5083 Al Alloy Sheet, *Metall. Mater. Trans. A*, 1996, **27A**, p 1889
25. R.M. Cleveland, A.K. Ghosh, and J.R. Bradley, Comparison of Superplastic Behavior in Two 5083 Aluminum Alloys, *Mat. Sci. Engi. A*, 2003, **A351**, p 228
26. Tallef et al., unpublished work, 2005
27. S. Kim and R. Verma, Effect of Copper Additions on Superplastic Behavior of 5083 Aluminum Alloy, MPMD Sixth Global Innovations Proceedings–Trends in Materials and Manufacturing Technologies for Transportation Industries, T.R. Bieler et al., Ed., TMS, Warrendale, PA, 2005, p 135–142
28. Metals Handbook, T. Lyman, Ed., American Society for Metals, 8th ed., Metals Park, OH, 1973